

Article

Evaluation of Empirical Daily Solar Radiation Models for the Northeast Coast of the Iberian Peninsula

Anton Vernet *  and Alexandre Fabregat

Department of Mechanical Engineering, Universitat Rovira i Virgili, Av. Països Catalans 26, 43007 Tarragona, Spain; alexandre.fabregat@urv.cat

* Correspondence: anton.vernet@urv.cat; Tel.: +34-977-559-685

Abstract: The ability to accurately predict daily solar radiation reaching the earth's surface is essential in applications such as solar power generation. Given their ease of use, many empirical models have been proposed based on different dependent variables such as cloud cover, daily temperature range, etc. In this study we evaluate 23 of these models for the prediction of daily solar radiation in the northern coastal zone of the Iberian Peninsula. Daily measurements during the period 2000–2018 from 16 meteorological stations spread over this area are used to adjust the parameters of each model, whose predictive capacity is then evaluated using measurements made between 2019 and 2022. Using different statistical metrics to assess their predictive performance, it was found that models based on hours of sunshine and level of cloudiness are significantly more accurate than those based on maximum and minimum daily temperature and day of the year. Specifically, the sunshine-based model by SBM3 obtained the highest Global Performance Indicator at 5.05. The results offer insight on the ability of each type of empirical model to accurately predict daily solar radiation in the Mediterranean region.

Keywords: solar radiation; empirical models; regression; Mediterranean area



Citation: Vernet, A.; Fabregat, A. Evaluation of Empirical Daily Solar Radiation Models for the Northeast Coast of the Iberian Peninsula. *Energies* **2023**, *16*, 2560. <https://doi.org/10.3390/en16062560>

Academic Editors: Maurizio De Lucia, Giacomo Pierucci, Francesco Taddei, Giuseppe Franchini and Giovanni Brumana

Received: 5 February 2023
Revised: 2 March 2023
Accepted: 7 March 2023
Published: 8 March 2023



Copyright: © 2023 by the authors. Licensee MDPI, Basel, Switzerland. This article is an open access article distributed under the terms and conditions of the Creative Commons Attribution (CC BY) license (<https://creativecommons.org/licenses/by/4.0/>).

1. Introduction

In a context of growing global energy demand, the sun is a clean and inexhaustible energy source that plays a central role in the generation of renewable power in relation to global warming mitigation and sustainable development. The harnessing of solar radiation, usually measured as the amount of radiant energy from the sun per square meter of the earth's surface, has driven major technological efforts in recent decades. The capacity to accurately predict the local solar radiation reaching the earth's surface is not only of interest for energy generation purposes but is also relevant in other fields, including architecture, urban development and agriculture. The understanding and modeling of many of the natural processes that take place in the troposphere, such as photosynthesis, evapotranspiration and cloud formation, depend on our ability to include correct estimates of solar radiation intensity in hydrological and plant growth models [1], and are also crucial in the design of new energy facilities. Remote satellite sensing makes it possible to obtain detailed information on solar irradiance, which is used, in combination with surface measurements, to develop mathematical models for estimating local surface radiation fluxes [2]. Due to significant maintenance costs and the need for frequent calibration, most meteorological stations do not have solar radiation measurement equipment, and direct measurements are scarce. In addition, data validity decays as distance from the measurement location increases, and data is considered unusable at distances greater than 50 km [3]. Over the years, different empirical mathematical models have been proposed to predict the solar radiation reaching a certain geographical area, depending on different factors such as the day of the year and/or meteorological parameters [4,5]. Extraterrestrial solar radiation can be accurately estimated using geometrical parameters, namely, the

relative distance between the sun and the earth (which depends on the day of the year) and the geographical location of the measurement point [6]. Obtaining the percentage of this radiative flux that travels through the atmosphere and reaches the earth's surface at a given time is somewhat more complicated, since it strongly depends on local atmospheric conditions. Therefore, models that uniquely depend on the day of the year, i.e., on the relative earth–sun position, typically fall short in providing reasonable estimations of surface solar radiation, and corrections accounting for local meteorological parameters are generally required. Regardless of their specific form and independent predictors, the goal of the empirical models is to provide reasonably accurate predictions of surface solar radiation using a small set of easily measured atmospheric variables. Although some global models provide acceptable results for large geographical areas [7], the applicability of most empirical models is restricted to relatively small regions. Some authors have carried out an exhaustive analysis of the multiple solar radiation models available in the literature. For instance, Mirzabe et al. [8] analyzed and classified up to 191 different models. By comparing different models for the estimation of solar radiation collected from around 90 scientific articles, Teke et al. [9] ranked them according to their accuracy. Similarly, Prieto and Garcia [10] reviewed a selection of 165 parametric models and quantified the solar prediction variability among them. These authors concluded that a high degree of complexity was not linked to increased accuracy. One of the most comprehensive reviews, conducted by Chen et al. [11], analyzed the predictive capabilities of 294 models and concluded that a universal model capable of accurately predicting local solar radiation for any location and environmental conditions is not yet available. Exploring further this trade-off between accuracy and complexity, which depends mainly on the purpose of the model and the availability of data, Besharat et al. [4] analyzed the performance of 78 different models and classified them into four categories according to meteorological input parameters, namely, sunshine-based, cloud-based, temperature-based and other meteorological-parameter-based models. A common feature of these four types of models is that they take into account latitude, solar declination, elevation, day length and atmospheric transmissivity by including extraterrestrial radiation in the model.

- Sunshine-based models. These models are based on daily sunshine duration. Although they allow accurate predictions of solar radiation, these models require data from specific equipment not present at many meteorological stations. Despotovic et al. [12] carried out an exhaustive analysis using 101 different sunshine-based models using data from 924 sites around the world. The authors concluded that although they could be used anywhere on the planet, their versatility was hindered by their limited accuracy.
- Cloud-based models. These models are based on daily measurements of average cloudiness. As with the sunshine-based models, many meteorological stations are not equipped with specific apparatus to measure cloudiness, and furthermore, such instruments are usually regarded as highly subjective. Ahamed et al. [13] made an exhaustive review of this type of model, concluding that they could be a good alternative for estimating solar radiation when sunshine hour data are not available.
- Temperature-based models. These models are usually based on daily maximum and minimum temperature values. Their major advantage is that these two quantities are measured by most meteorological stations.
- Other meteorological-parameter-based models. These models use a combination of several meteorological variables that often include the ratio of daily and maximum daily sunshine duration, relative humidity, air water content, average temperature, precipitation, etc.
- Day-of-year-based models. In addition to the four previous groups, there is a family of models based only on the day of the year. As they do not require meteorological data to characterize the atmospheric conditions, they are readily usable, although they offer predictions of limited accuracy compared to other model types.

The objectives of this study are to calibrate, validate and compare the daily solar radiation predictions obtained from a collection of methods representative of the different

types described above. For each model, the empirical coefficients will be fitted with data obtained from several meteorological stations scattered across the northeast of the Iberian Peninsula along the Mediterranean basin coast and the Balearic Islands. Models are categorized according to the classifications of Besharat et al. [4].

2. Materials and Methods

2.1. Study Area and Data

The region of interest spans the eastern part of the Iberian Peninsula, including the Catalan coast and the Balearic Islands, with local climates that are highly influenced by the proximity of the Mediterranean Sea. Data is retrieved from several meteorological stations scattered across this area, located at altitudes that, at most, barely exceed 1000 m above sea level, with an average value of 200 m. The climate is temperate and warm, with little rainfall in summer. The Köppen–Geiger climate classification of the area is mainly Csa, which corresponds to the Mediterranean climate [14]. Data from 12 meteorological stations located along 500 km of the Mediterranean coast of the Iberian Peninsula and 4 stations in the Balearic Islands were analyzed. Table 1 lists the name and location of the 16 stations, which are depicted on a map in Figure 1. In this study we considered meteorological data between the years 2000 to 2022, retrieved from the European Climate Assessment & Dataset project database [15].

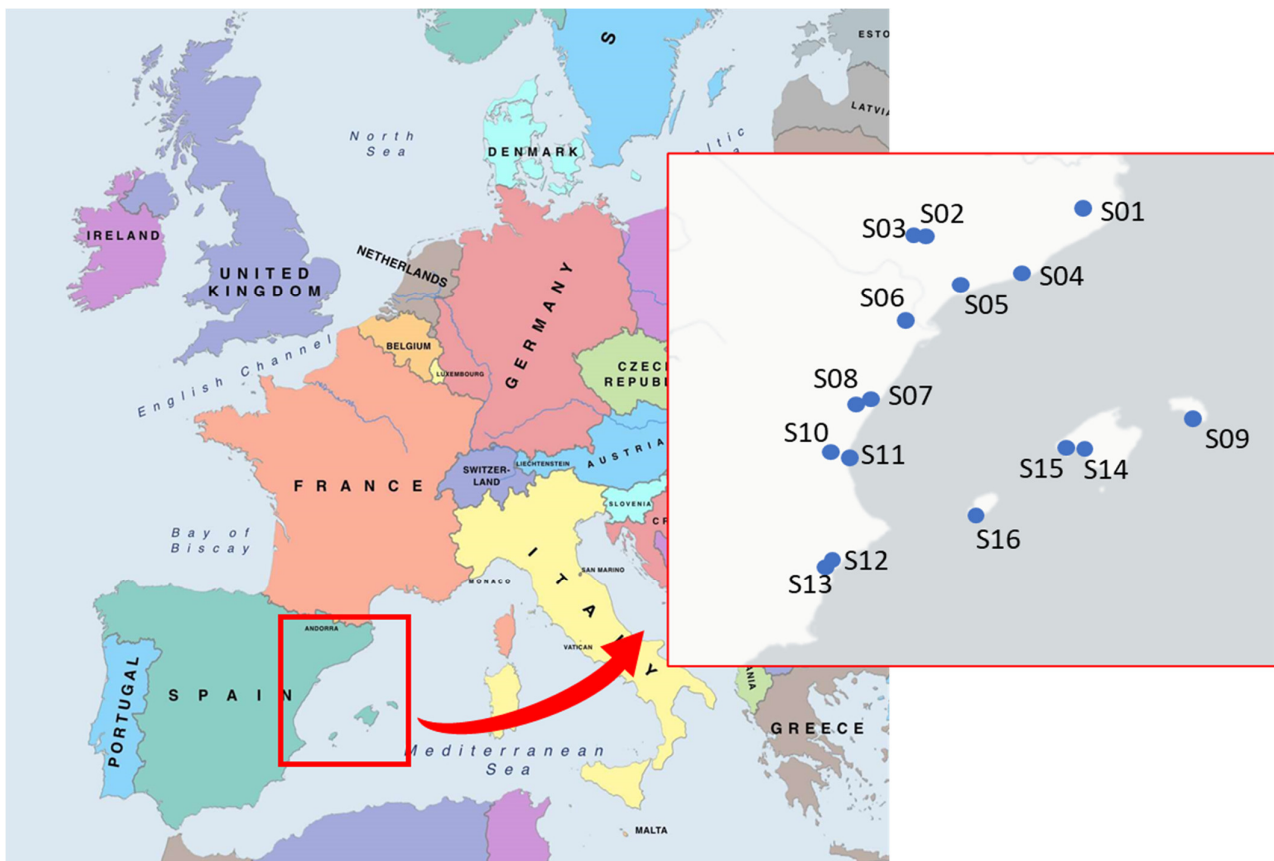


Figure 1. Geographical area studied and location of measuring stations. Map obtained from <https://mapswire.com/> (accessed on 6 March 2023).

Table 2 shows the annual daily mean values of some of the key meteorological variables used in the calculation of solar radiation for each station for the period between 2000 and 2022. The average annual temperature is 16.5 °C, with values ranging from slightly negative to over 36 °C in the summertime. The observed average annual rainfall is slightly less than 300 mm and the average relative humidity is 68%. The mean daily global solar irradiation

is $16.5 \text{ MJ}\cdot\text{m}^{-2}\cdot\text{day}^{-1}$. The mean annual daily sunshine hours of the region is 7.9 h, with a maximum around 14 h occurring in summer.

Table 1. Weather stations used and their location.

Station Name	Station ID	Latitude	Longitude	Elevation (m)
GIRONA/COSTA BRAVA	S01	41.91167	2.763056	143
LLEIDA	S02	41.62556	0.595	192
LLEIDA-AJUNTAMENT	S03	41.61639	0.583056	169
BARCELONA/AIRPORT	S04	41.29278	2.069722	4
REUS/AIRPORT	S05	41.14944	1.178889	71
TORTOSA—OBSERVATORIO DEL EBRO	S06	40.82056	0.491389	44
CASTELLON DE LA PLANA	S07	39.98917	0.040556	25
CASTELLON	S08	39.95	0.071389	35
MENORCA/MAO	S09	39.85444	4.215556	91
VALENCIA/AEROPUERTO	S10	39.48667	0.473056	69
VALENCIA	S11	39.48056	0.366389	11
ALICANTE	S12	38.3725	0.494167	81
ALICANTE EL ALTET	S13	38.28278	0.570556	43
PALMA DE MALLORCA/SON SAN JUAN	S14	39.56056	2.736667	8
PALMA DE MALLORCA CMT	S15	39.55556	2.626389	3
IBIZA/ESCODOLA	S16	38.87639	1.384167	6

Table 2. Annual meteorological averages of some variables at each study station.

Station ID	T Max (°C)	T Min (°C)	T Mean (°C)	Precipitation (mm)	Humidity (%)	Daily Solar Radiation ($\text{MJ m}^{-2} \text{Day}^{-1}$)	Sunshine Hours (h)
S01	37.0	−5.9	15.3	405.5	71.3	14.8	7.2
S02	38.8	−5.6	16.2	227.2	66.5	17.0	8.4
S03	38.0	−5.6	15.9	217.6	—	17.0	8.4
S04	33.1	−0.1	17.1	315.8	68.1	15.8	6.8
S05	35.8	−4.0	16.6	269.4	66.5	16.0	7.7
S06	38.4	−0.8	18.5	315.8	64.6	15.9	7.9
S07	35.8	1.5	18.2	263.9	—	16.7	8.2
S08	35.8	1.5	18.2	261.1	63.4	16.7	8.2
S09	34.3	1.9	17.6	412.9	74.1	15.9	7.4
S10	38.5	−1.8	18.1	239.1	63.0	16.9	8.2
S11	36.7	1.9	18.8	246.6	65.3	16.5	7.8
S12	36.5	0.6	18.7	212.7	67.4	17.7	8.5
S13	36.9	0.2	18.5	202.2	62.9	17.4	8.1
S14	37.7	−2.2	17.3	298.6	73.2	16.4	7.8
S15	35.0	3.2	18.8	342.1	73.6	16.6	8.0
S16	34.2	1.5	18.4	279.6	72.6	16.8	7.8
Mean	36.4	−0.8	17.6	281.9	68.0	16.5	7.9

2.2. Data Quality

To ensure the quality of the meteorological data (temperature, relative humidity, precipitation), all observations with invalid or spurious values were first removed. In the case of surface solar radiation values, the daily sky brightness index (K_T) has been used as a quality indicator. This parameter is defined as the ratio between the measured daily radiation and the extraterrestrial solar radiation. Jiang [16] recommends K_T values between 0.015 and 1.0. A value of $K_T = 0.015$ corresponds to a day with very intense cloudiness maintained throughout the day, while a value of $K_T = 1$ corresponds to a completely clear day with surface radiation equal to extraterrestrial radiation. Only data within the interval $0.015 \leq K_T \leq 1.0$ were considered. In addition, data with a daily insolation duration longer than the theoretical maximum duration have also been removed.

3. Modeling of Global Solar Radiation

3.1. Extraterrestrial Daily Global Solar Radiation

The amount of solar radiation reaching the upper layers of the atmosphere is well defined and can be calculated quite accurately from the relative positions of the sun and the earth (Julian day) and the geographic location of the point where the value of solar radiation is calculated. According to Duffie and Beckman [6], extraterrestrial solar radiation can be calculated as

$$H_o = \frac{24 \cdot 60}{\pi} G_{sc} \cdot d_r \cdot (w_s \cdot \sin \varphi \cdot \sin \delta + \cos \varphi \cdot \cos \delta \cdot \sin w_s) \quad (1)$$

where G_{sc} is the solar constant, φ is the latitude (rad), d_r is the inverse of the relative distance between the sun and the earth, δ is the solar declination and w_s is the sunset hour angle calculated as

$$w_s = \arccos(-\tan \varphi \cdot \tan \delta) \quad (2)$$

$$d_r = 1 + 0.033 \cdot \cos\left(\frac{2\pi}{365} J\right) \quad (3)$$

$$\delta = 0.409 \cdot \sin\left(\frac{2\pi}{365} J - 1.39\right) \quad (4)$$

where J is the Julian day.

Additionally, the maximum possible sunshine duration of the day is calculated as

$$S_o = \frac{2}{15} \cdot w_s \quad (5)$$

Due to absorption, reflection and scattering processes during its travel through the earth's atmosphere, the radiation that ultimately reaches the earth's surface is a fraction of the incoming solar radiation at the upper layers of the atmosphere. Figure 2 compares the variation of solar radiation at the earth's surface with extraterrestrial radiation at the REUS/AEROPORT site for the year 2018. It is observed that 20–30% of the extraterrestrial radiation does not reach the earth's surface. This reduction of radiation increases under adverse meteorological conditions, especially in the presence of high cloud cover. Since it accounts for the variability due to the relative positions of the earth and the sun through the year, the value of extraterrestrial solar radiation is an input parameter of most empirical models.

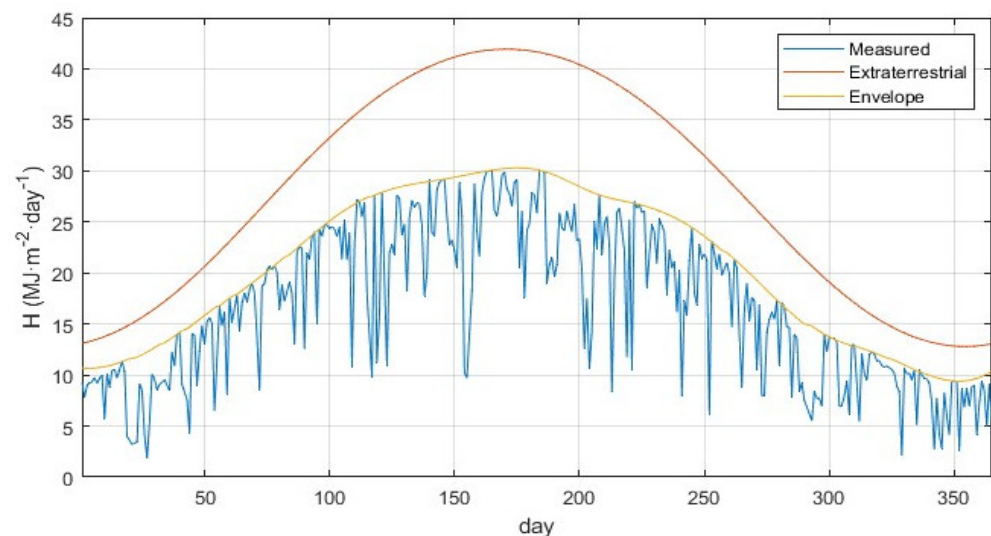


Figure 2. Comparison between the extraterrestrial radiation and the radiation registered on the earth's surface at the REUS/AIRPORT station (S05) during 2018.

3.2. Empirical Models for Estimation of Solar Radiation

In recent years, many empirical correlations have been developed to determine the amount of solar radiation reaching the earth’s surface based on different geographical and atmospheric parameters. Several publications exhaustively collect and classify a vast number of models according to the variables used in the calculation of daily solar radiation [4,8,10]. In this study, we compared the accuracy of some of the most well-known methodologies to compute local solar radiation in the Mediterranean area of the north-east region of the Iberian Peninsula. The models considered here belong to any of the following five categories: (1) day-of-the-year models, (2) sunshine-based models, (3) cloud-based models, (4) temperature-based models and (5) other meteorological-parameter-based models. The selection criteria took into account measurement availability, model simplicity, and previously reported performance. Except for the model of Garipey [17], all 23 models considered here depend on several coefficients fitted using measurements of meteorological variables. Garipey’s model directly uses precipitation and temperature information to calculate daily solar radiation with no need to fit any parameters by regression. As stated, all models except day-of-the-year-based ones include extraterrestrial radiation as an input, and therefore implicitly account for site latitude, solar declination and day length [4].

3.2.1. Day-of-the-Year-Based Models (DYBs)

As Figure 2 shows, daily solar radiation is a quasi-periodic yearly phenomenon [18]. Thus, these models assume that solar radiation can be readily estimated for each day of the year. This methodology is thought to be the simplest approach, with only one parameter required to get an estimation of the daily average solar radiation for a given location on the earth’s surface. Despite their simplicity, the impact of local meteorological conditions that may significantly affect the amount of radiation reaching the surface is not accounted for, and their accuracy often decreases under cloudy conditions. Table 3 lists the five models based on the day of the year considered in this study.

Table 3. Models based on day of the year used in this study.

Model ID	Model Equations	Reference
DYB1	$H = a + b \cdot \cos\left(\frac{2\pi}{364} \cdot J + c\right)$	[19]
DYB2	$H = a + b \cdot \sin\left(c \cdot \frac{2\pi}{365} \cdot J + d\right) + e \cdot \cos\left(f \cdot \frac{2\pi}{365} \cdot J + g\right)$	[20]
DYB3	$H = a + b \cdot \exp\left[-0.5 \cdot \left(\frac{J-c}{d}\right)^2\right] + e \cdot \exp\left[-0.5 \cdot \left(\frac{J-f}{g}\right)^2\right]$	[21]
DYB4	$H = a + b \cdot \left \sin\left[\frac{\pi}{365} \cdot (J + 5)\right]\right ^{1.5}$	[22]
DYB5	$H = a + \sum_{n=1}^2 b_n \cdot \cos\left(n \cdot \frac{2\pi}{365} \cdot J\right) + c_n \cdot \sin\left(n \cdot \frac{2\pi}{365} \cdot J\right)$	[23]

3.2.2. Sunshine-Based Models (SBMs)

As shown in Figure 3, solar radiation is highly correlated with hours of sunshine. This figure shows radiation at the earth’s surface, normalized by extraterrestrial radiation (H/H_0) as a function of normalized sunshine hours and S/S_0 for an arbitrary location in the region of interest. The significant correlation between the variables suggests that under unfavorable meteorological conditions (for example, high humidity or a cloudy day) associated with low values of S/S_0 , the amount of radiative energy arriving at the earth’s surface decreases.

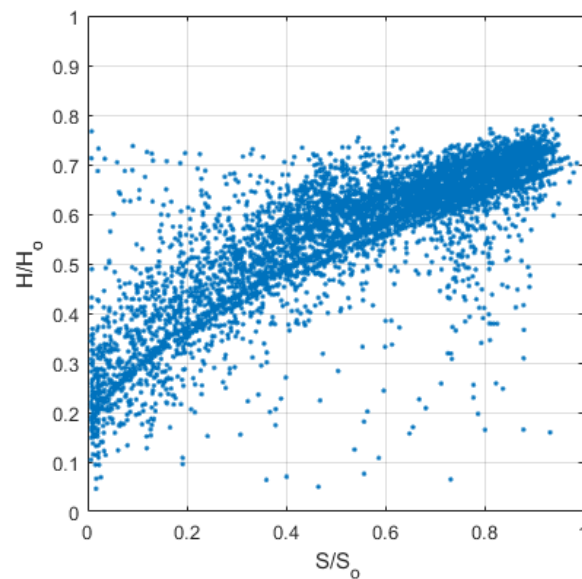


Figure 3. Variation of measured solar radiation and sunshine hours of the day at BARCELONA/AIRPORT station (S04) for the period 2000 to 2018.

Solar radiation calculation models based on the S/S_0 ratio exploit this relatively strong correlation and are among the most popular, along with those based on temperature [24]. The Angstrom-Prescott model [25] is one of the simplest and most widely used methods. This model is a modification of the Angstrom model [26] in which the use of clear sky radiation is replaced by extraterrestrial radiation. Several authors have modified the basic linear form of this model by extending it with higher order polynomial terms and also exponential and logarithmic forms.

The main drawback of this type of model (see the list of those considered in this study in Table 4) is the need to know the length of the solar day, the measurement of which requires specific equipment not available at all weather stations.

Table 4. Sunshine-based models used in this study.

Model ID	Model Equations	Reference
SBM1	$\frac{H}{H_0} = a + b \cdot \frac{S}{S_0}$	[25]
SBM2	$\frac{H}{H_0} = a + b \cdot \frac{S}{S_0} + c \cdot \left(\frac{S}{S_0}\right)^2$	[27]
SBM3	$\frac{H}{H_0} = a + b \cdot \frac{S}{S_0} + c \cdot \left(\frac{S}{S_0}\right)^2 + d \cdot \left(\frac{S}{S_0}\right)^3$	[28]
SBM4	$\frac{H}{H_0} = \exp(a) \cdot \left(\frac{S}{S_0}\right)^b$	[29]
SBM5	$\frac{H}{H_0} = a + b \cdot \log\left(\frac{S}{S_0}\right)$	[30]

3.2.3. Cloud-Based Models (CBMs)

As discussed above, the number of daily hours of sunshine is a meteorological parameter that is highly correlated with total daily solar irradiance. When insolation measurements are not available, CBMs estimate the solar radiation using the cloud cover. The total cloud cover index is often estimated by eye and reported in octas, with 0 corresponding to clear sky and 8 to overcast conditions [31]. Ahamed et al. [13] presented a comprehensive review of cloud-cover-based models and analyzed the hourly variation of solar radiation. Table 5 shows the cloud-cover-based models considered in this study.

Table 5. Cloud-cover-based models used in this study.

Model ID	Model Equations	References
CBM1	$\frac{H}{H_0} = a + b \cdot CC$	[32]
CBM2	$\frac{H}{H_0} = a + b \cdot CC + c \cdot (CC)^2$	[32,33]
CBM3	$\frac{H}{H_0} = a + b \cdot CC + c \cdot (CC)^2 + d \cdot (CC)^3$	[32]

3.2.4. Temperature-Based Models (TBMs)

Temperature-based models use maximum and minimum daily temperatures to estimate the daily solar radiation for a specific site. This type of methodology assumes that temperature difference can be used as a proxy for cloudiness [34]. Clear skies increase maximum temperature due to higher shortwave radiation, and the temperature minimum is lower due to higher transmissivity [35]. Thus, clear skies indicate higher temperature differences, while cloudy skies imply lower values for temperature changes. Notably, variations in temperature are also affected by many other factors than cloudiness, such as precipitation, wind velocity, elevation, soil evaporation, etc. Therefore, this type of method can exhibit significant levels of uncertainty and prediction error [34]. Recently, Qiu et al. [36] presented an extensive review of 82 models for computing daily solar radiation based solely on temperature data, along with 4 new proposed models. Their results were found to provide reasonable accuracy when used in different geographical zones across China. Mohammadi and Moazenzadeh [37] analyzed daily solar radiation estimates from 13 Peruvian meteorological stations using 7 empirical temperature-based models and proposed a new model for the stations using precipitation and relative humidity as additional variables. These models were developed on the basis of multiple linear regression analysis. They found that the empirical temperature-based models usually overestimate solar radiation at most of the stations. In the present study, the TBMs considered are listed in Table 6.

Table 6. Temperature-based models used in this study.

Model ID	Model Equations	Reference
TBM1	$\frac{H}{H_0} = a \sqrt{(T_{max} - T_{min})}$	[38]
TBM2	$H = a \sqrt{(T_{max} - T_{min})} \cdot H_0 + b$	[39]
TBM3	$\frac{H}{H_0} = a \cdot T_{max} + b \cdot T_{min} + c$	[40]
TBM4	$H = (a \cdot T_{max} + b \cdot T_{min}) \cdot H_0 + c$	[41]
TBM5	$\frac{H}{H_0} = a \cdot (1 - \exp(-b \cdot (T_{max} - T_{min})^c))$	[42]

3.2.5. Other Meteorological-Parameter-Based Models (OPMs)

Unlike the previous models, which are based on a single meteorological parameter, the five methods in Table 7 combine several parameters in an attempt to improve the prediction of solar radiation. The two first models (OPM1 and OPM2) combine daily sunshine hour duration and relative humidity data. Methods OPM3 and OPM5 use daily sunshine hour duration along with mean daily temperature. OPM3 also combines relative humidity to estimate the atmospheric precipitable water vapor per unit volume of air using the expression presented by [43]. OPM5 is a modification of the Angström-Preseott model [25] that adds data on mean temperature and precipitation. OPM4 uses only the maximum and minimum daily temperature and precipitation.

Table 7. Other meteorological-parameter-based models used in this study.

Model ID	Model Equations	References
OPM1	$\frac{H}{H_o} = a \cdot \left(\frac{S}{S_o}\right)^b \cdot RH^c$	[44]
OPM2	$\frac{H}{H_o} = a + b \cdot \frac{S}{S_o} + c \cdot RH$	[44]
OPM3	$\frac{H}{H_o} = a + b \cdot \frac{S}{S_o} + c \cdot W$ $W = 0.0049 \cdot RH * \left(\frac{\exp(26.23 - 5416/T_{mean})}{T_{mean}}\right)$	[43,45]
OPM4	$H = a \cdot H_o (T_{max} - T_{min})^{0.5} + b \cdot T_{max} + c * PPT + d \cdot PPT^2 + e$	[39]
OPM5	$\frac{H}{H_o} = a + b \cdot \frac{S}{S_o}$ $a = 0.3791 - 0.0041 \cdot T_{mean} - 0.0176 \cdot PPT$ $b = 0.4810 + 0.0043 \cdot T_{mean} - 0.0097 \cdot PPT$ (PPT in cm)	[17]

3.3. Statistical Performance Validation

To assess the performance of the models in Tables 3–7 on the dataset described in Section 2.1, we used up to nine statistical quantitative indicators. It should be noted that to ensure independent validation of the models, they were fitted using meteorological data from 2000 to 2018 and then tested with measurements taken between 2019 and 2022. The quantitative indicators used were:

1. Mean absolute error or MAE ($\text{MJ m}^{-2} \text{ day}^{-1}$) is a statistical indicator used to determine how close the calculated values are to the measurements. It is the sum of the absolute value of the differences between the measured values and the calculated values, divided by the number of measures. Performance increases as this metric tends toward zero.

$$\text{MAE} = \frac{1}{n} \sum_{i=1}^n |H_{m,i} - H_{c,i}| \quad (6)$$

2. Root mean square error or RMSE ($\text{MJ m}^{-2} \text{ day}^{-1}$) is often used in the literature, although some authors have expressed concerns about its suitability for this type of analysis given the large impact that a small set of large-discrepancy measurements can have on this metric, which uses the square of the difference between observed and predicted values [46].

$$\text{RMSE} = \sqrt{\frac{1}{n} \sum_{i=1}^n (H_{m,i} - H_{c,i})^2} \quad (7)$$

3. The mean absolute relative error or MARE is calculated as the sum of the absolute value of the relative differences between the measured and calculated data. Some authors express it as a percentage. The lower this value is, the better the model performance.

$$\text{MARE} = \frac{1}{n} \sum_{i=1}^n \left| \frac{H_{m,i} - H_{c,i}}{H_{m,i}} \right| \quad (8)$$

4. Uncertainty at 95% or U_{95} puts the emphasis on model deviation. For the standard normal distribution, a value of 1.96 implies that there is a 95% probability that a standard normal variable will fall between -1.96 and 1.96 [47]. SD is the standard deviation of the difference between calculated and measured solar radiation data.

$$U_{95} = 1.96 \cdot \sqrt{SD^2 + RMSE^2} \quad (9)$$

5. Root mean squared relative error or RMSRE is often preferred over the RMSE, although it is more sensitive to very low observation values [48]. This metric score decreases as model performance improves.

$$RMSRE = \sqrt{\frac{1}{n} \sum_{i=1}^n \left(\frac{H_{m,i} - H_{c,i}}{H_{m,i}} \right)^2} \quad (10)$$

6. Relative root mean squared error or RRMSE. According to Li et al. [40] and Despotovic et al. [12], the model can be considered excellent if RRMSE < 10%, good for 10% < RRMSE < 20%, weak for 20% < RRMSE < 30% and poor if RRMSE > 30%.

$$RRMSE = \frac{\sqrt{\frac{1}{n} \sum_{i=1}^n (H_{m,i} - H_{c,i})^2}}{\sum_{i=1}^n H_{m,i}} \cdot 100 \quad (11)$$

7. Mean bias error or MBE is used to quantify the tendency of the model to overestimate or underestimate the measured values. This indicator may not be an appropriate metric when simultaneously overestimated and underestimated values can cancel each other out.

$$MBE = \frac{1}{n} \sum_{i=1}^n (H_{m,i} - H_{c,i}) \quad (12)$$

8. The coefficient of determination or R^2 is frequently used in statistics to estimate how well model predictions capture trends in the observed data. Bounded between 0 and 1, the larger the value of R^2 the better the model performance.

$$R^2 = 1 - \frac{\sum_{i=1}^n (H_{m,i} - H_{c,i})^2}{\sum_{i=1}^n (H_{m,i} - H_m)^2} \quad (13)$$

9. The maximum absolute relative error or errMAX uses the largest relative difference between predicted and observed values.

$$errMax = \max \left(\left| \frac{H_{m,i} - H_{c,i}}{H_{m,i}} \right| \right) \quad (14)$$

Each of the indicators listed above can measure different aspects of the similarity between modeled and observed data. For this reason, it may be difficult to rank the different models using each of the indicators separately [8]. To ameliorate the limitations of model assessment based on individual scores, Behar et al. [47] defined the Global Performance Indicator (GPI), which Despotovic et al. [12] later modified and expressed as

$$GPI_i = \sum_{j=1}^m \alpha_j \cdot (\tilde{y}_j - y_{ij}) \quad (15)$$

where α_j is equal to 1 for all indicators except for R^2 , for which it takes the value of -1 , y_j is the median of scaled values of indicator j , and y_{ij} is the scaled value of indicator j for model i . The higher the value of GPI, the better the model performance in predicting daily terrestrial solar radiation.

4. Results and Discussion

Figure 4 schematically shows the methodology of the present study. The fitting parameters of the 23 models selected in this study were adjusted to obtain the best prediction

of daily solar radiation in the Mediterranean area of the Iberian Peninsula using daily meteorological data obtained between 2000 and 2018 from 16 measurement stations. The entire dataset for all the stations was used to determine each model regression coefficient. Separate fits for each station were not considered.

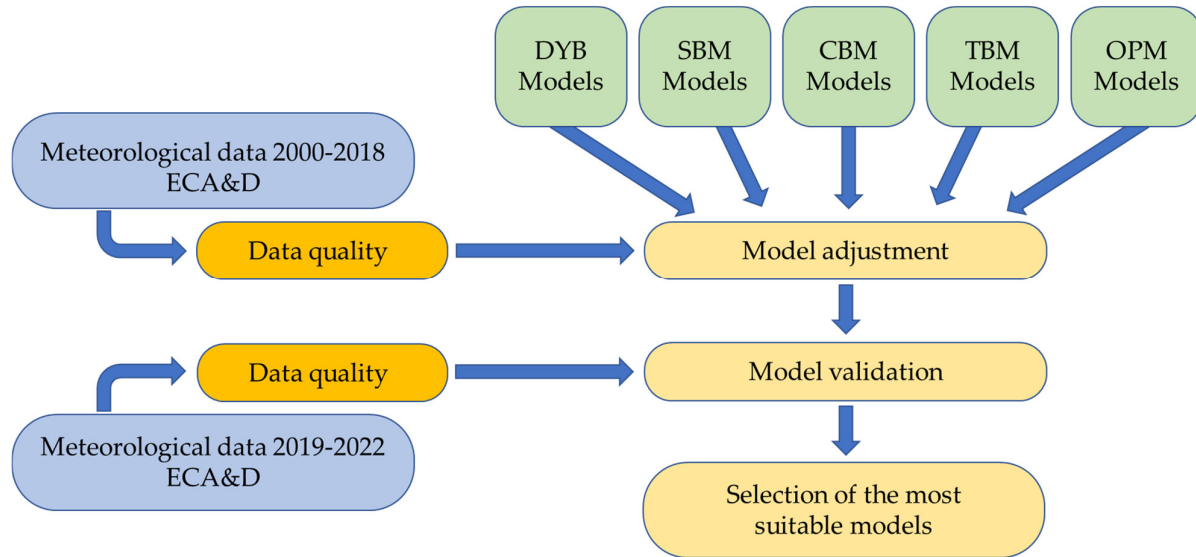


Figure 4. Working process followed in this study.

Table 8 shows the results for each model. Predictive accuracy is similar to that reported in the literature [4,12].

Table 8. Regression coefficients for each of the models tested.

Model ID	Model Equations	a	b	c	d	e	f	g
SBM1	$\frac{H}{H_0} = a + b \cdot \frac{S}{S_0}$	0.283	0.457					
SBM2	$\frac{H}{H_0} = a + b \cdot \frac{S}{S_0} + c \cdot \left(\frac{S}{S_0}\right)^2$	0.233	0.714	-0.238				
SBM3	$\frac{H}{H_0} = a + b \cdot \frac{S}{S_0} + c \cdot \left(\frac{S}{S_0}\right)^2 + d \cdot \left(\frac{S}{S_0}\right)^3$	0.223	0.829	-0.508	0.173			
SBM4	$\frac{H}{H_0} = \exp(a) \cdot \left(\frac{S}{S_0}\right)^b$	-0.378	0.333					
SBM5	$\frac{H}{H_0} = a + b \cdot \log\left(\frac{S}{S_0}\right)$	0.670	0.147					
TBM1	$\frac{H}{H_0} = a \sqrt{(T_{max} - T_{min})}$	0.182						
TBM2	$H = a \sqrt{(T_{max} - T_{min})} \cdot H_0 + b$	0.174	0.986					
TBM3	$\frac{H}{H_0} = a \cdot T_{max} + b \cdot T_{min} + c$	0.019	-0.015	0.339				
TBM4	$H = (a \cdot T_{max} + b \cdot T_{min}) \cdot H_0 + c$	0.026	-0.013	4.14				
TBM5	$\frac{H}{H_0} = a \cdot (1 - \exp(-b \cdot (T_{max} - T_{min})^c))$	0.673	0.220	0.990				
DYB1	$H = a + b \cdot \cos\left(\frac{2\pi}{364} \cdot J + c\right)$	16.60	-8.970	0.159				
DYB2	$H = a + b \cdot \sin\left(c \cdot \frac{2\pi}{365} \cdot J + d\right) + e \cdot \cos\left(f \cdot \frac{2\pi}{365} \cdot J + g\right)$	16.08	-9.259	-0.95	-5.03	0.21	-11.03	7.88

Table 8. Cont.

Model ID	Model Equations	a	b	c	d	e	f	g
DYB3	$H = a + b \cdot \exp \left[-0.5 \cdot \left(\frac{J-c}{d} \right)^2 \right] + e \cdot \exp \left[-0.5 \cdot \left(\frac{J-f}{g} \right)^2 \right]$	31.16	-140.20	164.15	164.06	134.50	165.93	-131.34
DYB4	$H = a + b \cdot \left \sin \left[\frac{\pi}{365} \cdot (J + 5) \right] \right ^{1.5}$	6.16	18.69					
DYB5	$H = a + \sum_{n=1}^2 b_n \cdot \cos \left(n \cdot \frac{2\pi}{365} \cdot J \right) + c_n \cdot \sin \left(n \cdot \frac{2\pi}{365} \cdot J \right)$	16.57	-8.862	1.509	-0.356	0.503		
CBM1	$\frac{H}{H_0} = a + b \cdot CC$	0.724	-0.042					
CBM2	$\frac{H}{H_0} = a + b \cdot CC + c \cdot (CC)^2$	0.675	0.00305	-0.00621				
CBM3	$\frac{H}{H_0} = a + b \cdot CC + c \cdot (CC)^2 + d \cdot (CC)^3$	0.673	0.00751	-0.00777	0.00014			
OPM1	$\frac{H}{H_0} = a \cdot \left(\frac{S}{S_0} \right)^b \cdot RH^c$	1.007	0.324	-0.094				
OPM2	$\frac{H}{H_0} = a + b \cdot \frac{S}{S_0} + c \cdot RH$	0.321	0.445	-0.00046				
OPM3	$\frac{H}{H_0} = a + b \cdot \frac{S}{S_0} + c \cdot W$	0.285	0.453	-0.00032				
OPM4	$H = a \cdot H_0 (T_{max} - T_{min})^{0.5} + b \cdot T_{max} + c \cdot PPT + d \cdot PPT^2 + e$	0.148	0.184	-0.290	0.002	-0.694		
OPM5	$\frac{H}{H_0} = a + b \cdot \frac{S}{S_0}$	Parameters do not need to be adjusted and are a function of T_{mean} and PPT						

The coefficients obtained for each model cannot be compared directly with those existing in the literature, since most authors adjust the models to a specific geographical area that does not coincide with the one studied in this study. However, a comparison has been made between the values obtained by other authors and those found in this study. For some of the models based on sunshine hours, Besharat et al. [4] collected values of the coefficients obtained for different worldwide geographical locations. For example, for the Angstrom-PreScott model (SBM1), these authors report 36 results, of which 2 present negative values of the coefficient a that do not conform to those obtained by the majority of authors. For the rest of the cases analyzed, the values of coefficient a are between 0.133 and 0.367, with a mean value of 0.256, while the values of coefficient b are between 0.311 and 0.696, with a mean value of 0.495. The mean values for this model are very close to those obtained in our study ($a = 0.283$ and $b = 0.457$). These results are also in good agreement with those reported by Page [49], who claimed the model to be usable anywhere in the world with regression coefficients $a = 0.23$ and $b = 0.48$. For the other models studied, it has been found that the value of the regression coefficients calculated in this study is of the same order of magnitude as that observed in most of the literature consulted.

Each model and their respective parameters in Table 8 was used to predict the daily solar radiation for the years 2019 to 2022. Table 9 shows, for each model, all the performance scores computed using the predicted and measured values of daily solar radiation. The most accurate scores are highlighted in bold type. Smaller values of each score are associated with improved predictive capabilities, except for R^2 and GPI. A value of 0 for the coefficient of determination (R^2) indicates no linear relationship between the predicted and observed values, while a value of 1 corresponds to a perfect linear relationship. Regarding the upper unbounded Global Performance Indicator (GPI), the higher the GPI the better the model's predictive capabilities.

Table 9. Statistical indicators for the empirical models. The most accurate scores are highlighted in bold type.

	MAE	RMSE	MARE	U ₉₅	MRSRE	RRMSE	MBE	R ²	errMax	GPI
SBM1	1.23	2.32	0.101	6.42	0.268	13.78	0.050	0.909	6.264	4.814
SBM2	1.20	2.31	0.093	6.40	0.260	13.75	0.120	0.909	5.061	5.002
SBM3	1.19	2.31	0.092	6.39	0.259	13.73	0.110	0.910	4.827	5.048
SBM4	1.46	2.40	0.108	6.62	0.258	14.30	0.369	0.902	3.393	4.673
SBM5	1.70	2.61	0.134	7.22	0.293	15.54	0.287	0.884	3.737	3.822
TBM1	3.01	3.98	0.226	10.97	0.399	23.68	0.568	0.731	13.410	−1.752
TBM2	2.97	3.94	0.233	10.93	0.422	23.50	2.64×10^{-1}	0.735	13.620	−1.722
TBM3	2.74	3.62	0.224	10.03	0.421	21.59	0.304	0.776	13.734	−0.827
TBM4	2.88	3.83	0.232	10.61	0.425	22.80	1.28×10^{-1}	0.751	13.584	−1.353
TBM5	2.80	3.69	0.223	10.17	0.419	21.97	0.548	0.769	13.991	−1.080
DYB1	3.13	3.99	0.261	11.01	0.489	23.73	5.10×10^{-1}	0.729	14.093	−2.437
DYB2	3.13	4.00	0.261	11.05	0.489	23.82	5.14×10^{-1}	0.728	14.123	−2.478
DYB3	3.15	4.03	0.264	11.12	0.495	23.95	0.478	0.724	13.922	−2.556
DYB4	3.20	4.07	0.267	11.24	0.492	24.23	5.34×10^{-1}	0.718	15.072	−2.813
DYB5	3.12	4.00	0.260	11.05	0.490	23.80	4.79×10^{-1}	0.728	14.583	−2.494
CBM1	1.90	2.87	0.157	8.19	0.335	19.58	0.385	0.841	11.011	1.821
CBM2	1.86	2.85	0.149	8.10	0.318	19.42	0.472	0.844	10.910	2.000
CBM3	1.86	2.85	0.149	8.10	0.318	19.42	0.470	0.844	10.872	2.000
OPM1	1.30	2.28	0.097	6.50	0.245	15.48	0.297	0.899	3.365	4.855
OPM2	1.12	2.22	0.092	6.36	0.258	15.06	0.043	0.904	6.263	4.881
OPM3	1.13	2.22	0.093	6.37	0.259	15.10	0.061	0.904	6.293	4.847
OPM4	2.83	3.77	0.220	10.46	0.386	22.48	1.80×10^{-1}	0.758	7.444	−0.479
OPM5	2.84	3.65	0.209	8.86	0.356	21.73	−2.486	0.774	4.792	1.348

Although, as shown in Figure 3, the relationship between solar radiation and the fraction of sunshine hours has been found to be non-linear [50], the performance score results suggest that the linear Angstrom-Prescott model (SBM1) provides reasonably good estimates, as do the rest of the SBMs. Regarding MAE, RMSE and U₉₅, the best model for this geographical region is OPM2, with values of MAE = 1.12 MJ·m^{−2}·day^{−1}, RMSE = 2.22 MJ·m^{−2}·day^{−1} and U₉₅ = 6.36 MJ·m^{−2}·day^{−1}. This model is an Angstrom-Prescott model with an additional parameter accounting for relative humidity. The models OPM2 and SBM3 are the best according to the values of the mean absolute relative error (MARE = 0.092) but are very close to OPM3 and SBM2 (MARE = 0.093). The smallest root mean squared relative error (RMSRE = 0.245) and the maximum absolute relative error (errMax = 3.365) correspond to OPM1, a model that also uses daily sunshine hours and relative humidity as input parameters. The third order equation based on daily sunshine hours (SBM3) is considered the best regarding RRMSE (13.73%) and R² (0.91). The only statistical indicator that points to a model not based on sunshine hours is the mean bias error. In this case, the model with an MBE close to zero is TBM4 (MBE = 0.128 MJ·m^{−2}·day^{−1}). Several models might seem to offer good predictions of solar radiation given the near-zero values of this metric, but this statistical parameter does not allow discriminating between small deviations and large deviations of similar magnitude but opposite sign.

The value of the GPI also indicates that sunshine-based models perform best for values ranging between 3.82 and 5.04. Good performance is also found for OPM1, OPM2 and OPM3. While OPM2 and OPM3 are modified versions of the Angstrom-Prescott model that include relative humidity and atmospheric precipitable water per unit volume of air, respectively, the OPM1 model uses the fraction of sunshine hours and relative humidity.

This suggests that adding other meteorological variables to the models based on sunshine hours has a limited impact on model performance. Cloud-cover-based models perform slightly worse than SBMs, but still offer better predictions than the rest of the methods considered in this study. As previously reported [51], the models based on temperature (TBMs) and day of the year (DYBs) are found to be less accurate. The GPI values for this type of models are all negative, since for all statistical indicators it was found that their performance is worse than the median of the rest of the models. Among these, the present results found TBM3 [40] to be the best-performing temperature-based model. The models based on the day of the year (DYBs), with no input from local meteorology, exhibit the overall worst performance.

Despite differences between scores among all models considered in this study, the overall differences between them are relatively narrow. For instance, the R^2 score ranges between 0.72 and 0.91, suggesting that even the worst-performing model can provide reasonably good estimates of solar radiation depending on the trade-off between accuracy and data availability of the specific application.

To investigate model performance for each data collection site, we determined the GPI score for each meteorological station. The results in Figure 5 confirm that when analyzed separately, SBMs offer the best predictive capabilities, with the Angstrom-PreScott model (SBM1) offering the best predictions.

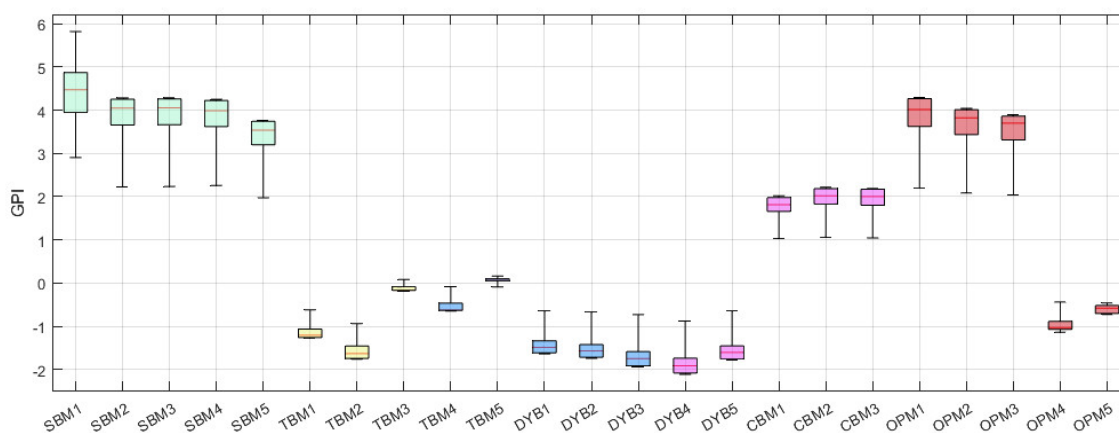


Figure 5. Distribution of GPI for each model, computed individually for each meteorological station.

5. Conclusions

Solar energy is a clean, renewable energy source that offers a sustainable alternative to the use of fossil fuels. Knowing the amount of solar radiation available in each geographical area is important for the design of solar energy production systems. Empirical models are the most widely used methods for obtaining such estimates of the solar radiation available at the earth's surface.

In this article, we focus on the area located on the Mediterranean slope of the Iberian Peninsula and the Balearic Islands. The accuracy of 23 different models for predicting daily solar radiation was analyzed. Depending on the variables used in the models, these were grouped into five different types, namely: (1) day of the year, (2) hours of sunshine, (3) cloudiness, (4) temperature and (5) other meteorological parameters. Based on meteorological data measured at 16 different sites between the years 2000 and 2018, the coefficients of each model were fitted by regression. The data set used to fit the models included all stations simultaneously to obtain unique coefficients for the entire geographical region of interest. The adjusted coefficients obtained were used to calculate daily solar radiation for the years 2019 to 2022. The predictive ability of each model was estimated using several scores quantifying the differences between the observed and predicted values. The Global Performance Indicator (GPI) was used to rank the models according to overall accuracy.

The models based on sunshine hours were found to be the most accurate, both when all stations were considered together and individually. In the latter case, we found that the classical Angstrom-Prescott model offers the best accuracy. The results suggest that adding other meteorological parameters such as relative humidity or precipitation to the models based on sunshine hours does not notably improve their performance. The OPM1, OPM2 and OPM3 models exhibit similar performance to those found for sunshine hour models. The models based on cloudiness offer slightly lower accuracy than those based on sunshine hours, with R^2 values around 0.85. The models based on temperature and day of the year exhibit the worst performance.

The analysis suggests that, when sunshine hour data are not available, cloudiness-based models should be used. In cases where cloudiness data are not available, models based on temperature or day of the year could be an alternative that would provide an acceptable estimate of solar radiation. Although not all the models available in the literature have been reviewed, the considered sample includes some of the most popular models that have been found to offer reasonably good predictions of daily solar radiation in the studied area.

The use of artificial intelligence and machine learning is an aspect to be considered in future research. The availability of massive data sets on meteorological conditions (cloudiness, temperature, relative humidity) for a large number of locations opens the possibility of using machine learning and artificial intelligence techniques to develop new modelling tools for the prediction of local radiative energy. Moazenzadeh et al. [52] compared different Support Vector Machine (SVM) algorithms for predicting daily solar radiation at seven meteorological stations in Iran. Almizamir et al. [53] conducted a comparative study of different machine learning models for solar radiation estimation in two geographical areas: the United States and Turkey. Geshnigan et al. [54] used 7 different artificial intelligence approaches for estimating daily solar radiation at 11 meteorological stations in Illinois (USA). Satellite measurements have also been used to derive new data-driven models for predicting local surface radiative energy flux. Mohammadi et al. [55] used ERA-Interim (ECMWF) datasets in the three geographical locations in Iran with promising results in terms of predictive accuracy.

Regarding our ongoing and future efforts, we want to take a step further and try to replace both the empirical and the standard ML-based approaches with interpretable closed-form mathematical models. To obtain them, we will feed massive datasets of daily solar radiation measurements into a “machine scientist” [56] tool to obtain models capable of capturing the physics of the problem without resorting to empirical approximations of limited generalization.

Author Contributions: A.V. and A.F. have contributed equally to the completion of the work presented and to the preparation, writing, and revision of the article. All authors have read and agreed to the published version of the manuscript.

Funding: This research has been financially supported by the Generalitat de Catalunya—AGAUR under the 2017 SGR 01234 project.

Data Availability Statement: The meteorological data for the years 2000 to 2022 used in this study are publicly available from the European Climate Assessment & Dataset project (<https://www.ecad.eu/> accessed on 6 March 2023) [15].

Conflicts of Interest: The authors declare no conflict of interest. The funders had no role in the design of the study, in the collection, analyses, or interpretation of data, in the writing of the manuscript, or in the decision to publish the results.

Nomenclature

a–g	Model regression coefficients
CC	Cloud cover index
d_r	The inverse of the relative distance between the sun and the earth
G_{sc}	Solar constant ($0.0820 \text{ MJ} \cdot \text{m}^{-2} \cdot \text{min}^{-1}$)

H	Daily global solar radiation ($\text{MJ m}^{-2} \text{ day}^{-1}$)
H_m	Measured daily global solar radiation ($\text{MJ m}^{-2} \text{ day}^{-1}$)
H_c	Calculated daily global solar radiation ($\text{MJ m}^{-2} \text{ day}^{-1}$)
H_o	Daily extraterrestrial radiation ($\text{MJ m}^{-2} \text{ day}^{-1}$)
J	Day of the year starting 1 January
K_T	Daily sky clearness index
PPT	Accumulated precipitation (mm)
R^2	Coefficient of determination
RH	Relative humidity
S	Daily sunshine duration (h)
S_o	Maximum possible daily sunshine duration (h)
T_{max}	Daily maximum temperature
T_{min}	Daily minimum temperature
T_{mean}	Daily mean temperature
U_{95}	Uncertainty at 95% ($\text{MJ m}^{-2} \text{ day}^{-1}$)
W	Atmospheric precipitable water per unit volume of air
w_s	Sunset hour angle (rad)
Greek Symbols	
δ	Solar declination (rad)
φ	Latitude (rad)
Acronyms	
ECMWF	European Centre for Medium-Range Weather Forecasts
errMAX	Maximum absolute relative error ($\text{MJ m}^{-2} \text{ day}^{-1}$)
GPI	Global Performance Indicator
MAE	Mean absolute error ($\text{MJ m}^{-2} \text{ day}^{-1}$)
MARE	Mean absolute relative error
MBE	Mean bias error. ($\text{MJ m}^{-2} \text{ day}^{-1}$)
RMSE	Root mean square error ($\text{MJ m}^{-2} \text{ day}^{-1}$)
RMSRE	Root mean squared relative error
RRMSE	Relative root mean squared error (%)
SD	Standard deviation

References

- Allen, R.G.; Pereira, L.S.; Raes, D.; Smith, M. *Crop Evapotranspiration. Guidelines for Computing Crop Water Requirements*; FAO Irrigation and Drainage Paper 56; Food and Agriculture Organization of the United Nations: Rome, Italy, 1998.
- Chen, Q.; Li, X.; Zhang, Z.; Zhou, C.; Guo, Z.; Liu, Z.; Zhang, H. Remote sensing of photovoltaic scenarios: Techniques, applications and future directions. *Appl. Energy* **2023**, *333*, 120579. [[CrossRef](#)]
- Younes, S.; Muneer, T. Comparison between solar radiation models based on cloud information. *Int. J. Sustain. Energy* **2007**, *26*, 121–147. [[CrossRef](#)]
- Besharat, F.; Dehghan, A.A.; Faghih, A.R. Empirical models for estimating global solar radiation: A review and case study. *Renew. Sustain. Energy Rev.* **2013**, *21*, 798–821. [[CrossRef](#)]
- Jahani, B.; Dinpashoh, Y.; Nafchi, A.R. Evaluation and development of empirical model for estimating daily solar radiation. *Renew. Sustain. Energy Rev.* **2017**, *73*, 878–891. [[CrossRef](#)]
- Duffie, J.A.; Beckman, W.A. *Solar Engineering of Thermal Processes*, 4th ed.; John Wiley & Sons: New York, NY, USA, 2013.
- Kaplanis, S.; Kumar, J.; Kaplani, E. On a universal model for the prediction of the daily global solar radiation. *Renew. Energy* **2016**, *91*, 178–188. [[CrossRef](#)]
- Mirzabe, A.H.; Hajiahmad, A.; Keyhani, A.; Mirzaei, N. Approximation of daily solar radiation: A comprehensive review on employing of regression models. *Renew. Energy Focus* **2022**, *41*, 143–159. [[CrossRef](#)]
- Teke, A.; Yıldırım, H.B.; Çelik, O. Evaluation and performance comparison of different models for the estimation of solar radiation. *Renew. Sustain. Energy Rev.* **2015**, *50*, 1097–1107. [[CrossRef](#)]
- Prieto, J.I.; Garcia, D. Global solar radiation models: A critical review from the point of view of homogeneity and case study. *Renew. Sustain. Energy Rev.* **2022**, *155*, 111856. [[CrossRef](#)]
- Chen, J.L.; He, L.; Yang, H.; Ma, M.H.; Chen, Q.; Wu, S.L.; Xiao, Z.L. Empirical models for estimating monthly global solar radiation: A most comprehensive review and comparative case study in China. *Renew. Sustain. Energy Rev.* **2019**, *108*, 91–111. [[CrossRef](#)]
- Despotovic, M.; Nedic, V.; Despotovic, D.; Cvetanovic, S. Review and statistical analysis of different global solar radiation sunshine models. *Renew. Sustain. Energy Rev.* **2015**, *52*, 1869–1880. [[CrossRef](#)]
- Ahamed, M.S.; Guo, H.; Tanino, K. Cloud cover-based models for estimation of global solar radiation: A review and case study. *Int. J. Green Energy* **2021**, *19*, 175–189. [[CrossRef](#)]

14. Beck, H.E.; Zimmermann, N.E.; McVicar, T.R.; Vergopolan, N.; Berg, A.; Wood, E.F. Present and future Köppen-Geiger climate classification maps at 1-km resolution. *Sci. Data* **2018**, *5*, 180214. [[CrossRef](#)] [[PubMed](#)]
15. Klein Tank, A.M.G.; Wijngaard, J.B.; Können, G.P.; Böhm, R.; Demarée, G.; Gocheva, A.; Mileta, M.; Pashiardis, S.; Hejkrlik, L.; Kern-Hansen, C.; et al. Daily dataset of 20th-century surface air temperature and precipitation series for the European Climate Assessment. *Int. J. Climatol.* **2002**, *22*, 1441–1453. [[CrossRef](#)]
16. Jiang, Y. Estimation of monthly mean daily diffuse radiation in China. *Appl. Energy* **2009**, *86*, 1458–1646. [[CrossRef](#)]
17. Gariépy, J. *Estimation of Global Solar Radiation*; International Report; Service of Meteorology, Government of Quebec: Montreal, QC, Canada, 1980.
18. Zeroual, A.; Ankrim, M.; Wilkinson, A.J. Stochastic modelling of daily global solar radiation measured in Marrakesh, Morocco. *Renew. Energy* **1995**, *6*, 787–793. [[CrossRef](#)]
19. Kaplanis, S.; Kaplani, E. A model to predict expected mean and stochastic hourly global solar radiation $I(h; n_j)$ values. *Renew. Energy* **2007**, *32*, 1414–1425. [[CrossRef](#)]
20. Li, H.; Ma, W.; Lian, Y.; Wang, X. Estimating daily global solar radiation by day of year in China. *Appl. Energy* **2010**, *87*, 3011–3017. [[CrossRef](#)]
21. Quej, V.H.; Almorox, J.; Ibrakhimov, M.; Saito, L. Estimating daily global solar radiation by day of the year in six cities located in the Yucatán Peninsula, Mexico. *J. Clean. Prod.* **2017**, *141*, 75–82. [[CrossRef](#)]
22. Bulut, H.; Büyükalaca, O. Simple model for the generation of daily global solar-radiation data in Turkey. *Appl. Energy* **2007**, *54*, 477–491. [[CrossRef](#)]
23. Rahoma, U.A.; Hassan, A.H. Fourier transforms investigation of global solar radiation at true noon: In the desert climatology. *Am. J. Appl. Sci.* **2007**, *4*, 902–907. [[CrossRef](#)]
24. Benti, N.E.; Aneseyee, A.B.; Asfaw, A.A.; Geffe, C.A.; Tiruye, G.A.; Mekonnen, Y.S. Estimation of global solar radiation using sunshine-based models in Ethiopia. *Cogent Eng.* **2022**, *9*, 2114200. [[CrossRef](#)]
25. Prescott, J.A. Evaporation from water Surface in relation to solar radiation. *Trans. R. Soc. Aust.* **1940**, *46*, 114–118.
26. Ångström, A. Solar and terrestrial radiation. *Q. J. R. Meteorol. Soc.* **1924**, *50*, 121–125. [[CrossRef](#)]
27. Ogelman, H.; Ecevit, A.; Tasdemiroglu, E. A new method for estimating solar radiation from bright sunshine data. *Sol. Energy* **1984**, *33*, 19–25. [[CrossRef](#)]
28. Bahel, V.; Bakhsh, H.; Srinivasan, R. A correlation for estimation of global solar radiation. *Energy* **1987**, *12*, 131–135. [[CrossRef](#)]
29. Coppolino, S. A new correlation between clearness index and relative sunshine. *Renew. Energy* **1994**, *4*, 417–423. [[CrossRef](#)]
30. Ampratwum, D.B.; Dorvlo, A.S.S. Estimation of solar radiation from the number of sunshine hours. *Appl. Energy* **1999**, *63*, 161–167. [[CrossRef](#)]
31. Badescu, V.; Dumitrescu, A. Simple solar radiation modelling for different cloud types and climatologies. *Theor. Appl. Clim.* **2016**, *124*, 141–160. [[CrossRef](#)]
32. Badescu, V. Correlations to estimate monthly mean daily solar global irradiation: Application to Romania. *Energy* **1999**, *24*, 883–893. [[CrossRef](#)]
33. Black, J.N. The Distribution of solar radiation over the earth's surface. *Arch. Meteorol. Geophys. Bioclimatol. Ser. B* **1956**, *7*, 165–1889.
34. Allen, R.G. Self-calibrating method for estimating solar radiation from air temperature. *J. Hydrol. Eng.* **1997**, *2*, 56–67. [[CrossRef](#)]
35. Almorox, J.; Bocco, M.; Willington, E. Estimation of daily global solar radiation from measured temperatures at Cañada de Luque, Cordoba, Argentina. *Renew. Energy* **2013**, *60*, 382–387. [[CrossRef](#)]
36. Qiu, R.J.; Li, L.A.; Wu, L.F.; Agathokleous, E.; Liu, C.W.; Zhang, B.Z.; Luo, Y.F.; Sun, S.L. Modeling daily global solar radiation using only temperature data: Past, development, and future. *Renew. Sustain. Energy Rev.* **2022**, *163*, 112511. [[CrossRef](#)]
37. Mohammadi, B.; Moazenzadeh, R. Performance Analysis of Daily Global Solar Radiation Models in Peru by Regression Analysis. *Atmosphere* **2021**, *12*, 389. [[CrossRef](#)]
38. Hargreaves, G.L.; Hargreaves, G.H.; Riley, P. Irrigation water requirement for the Senegal River Basin. *J. Irrig. Drain. Eng.* **1985**, *111*, 265–275. [[CrossRef](#)]
39. Hunt, L.A.; Kuchar, L.; Swanton, C.J. Estimation of solar radiation for use in crop modeling. *Agric. For. Meteorol.* **1998**, *91*, 293–300. [[CrossRef](#)]
40. Li, M.F.; Liu, H.B.; Guo, P.T.; Wu, W. Estimation of daily solar radiation from routinely observed meteorological data in Chongqing, China. *Energy Convers. Manag.* **2010**, *51*, 2575–2579. [[CrossRef](#)]
41. Li, M.-F.; Fan, L.; Liu, H.-B.; Guo, P.-T.; Wu, W. A general model for estimation of daily global solar radiation using air temperatures and site geographic parameters in Southwest China. *J. Atmos. Solar-Terr. Phys.* **2013**, *92*, 145–150. [[CrossRef](#)]
42. Bristow, C.L.; Campbell, G.S. On the relationship between incoming solar radiation and daily maximum and minimum temperature. *Agric. For. Meteorol.* **1984**, *31*, 159–166. [[CrossRef](#)]
43. Leckner, B. The spectral distribution of solar radiation at the earth's surface elements of a model. *Sol. Energy* **1978**, *20*, 143–150. [[CrossRef](#)]
44. Swartman, R.K.; Ogunlade, O. Solar radiation estimates from common parameters. *Sol. Energy* **1967**, *11*, 170–172. [[CrossRef](#)]
45. Garg, H.P.; Garg, S.T. Prediction of global solar radiation from bright sunshine hours and other meteorological parameters. In *Solar-India, Proceedings on National Solar Energy Convention*; Allied Publishers: New Delhi, India, 1982; pp. 1.004–1.007.
46. Willmott, C.J.; Matsuura, K. Advantages of the mean absolute error (MAE) over the root mean square error (RMSE) in assessing average model performance. *Clim. Res.* **2005**, *30*, 79–82. [[CrossRef](#)]

47. Behar, O.; Khellaf, A.; Mohammedi, K. Comparison of solar radiation models and their validation under Algerian climate—The case of direct irradiance. *Energy Convers. Manag.* **2015**, *98*, 236–251. [[CrossRef](#)]
48. Webber, H.; Martre, P.; Asseng, S.; Kimball, B.; White, J.; Ottman, M.; Wall, G.W.; De Sanctis, J.; Grant, R.; Kassie, B.; et al. Canopy temperature for simulation of heat stress in irrigated wheat in a semi-arid environment: A multi-model comparison. *Field Crops Res.* **2017**, *202*, 21–35. [[CrossRef](#)]
49. Page, J.K. The estimation of monthly mean values of daily total short-wave radiation on vertical and inclined surfaces from sunshine records for latitudes 40N–40S. In Proceedings of the UN Conference on New Sources of Energy, Rome, Italy, 16 May 1961; Volume 4, pp. 378–390.
50. Suehrcke, H.; Bowden, R.S.; Hollands, K.G.T. Relationship between sunshine duration and solar radiation. *Sol. Energy* **2013**, *92*, 160–171. [[CrossRef](#)]
51. Quej, V.H.; Almorox, J.; Ibrakhimov, M.; Saito, L. Empirical models for estimating daily global solar radiation in Yucatán Peninsula, Mexico. *Energy Convers. Manag.* **2016**, *110*, 448–456. [[CrossRef](#)]
52. Moazenzadeh, R.; Mohammadi, B.; Duan, Z.; Delghandi, M. Improving generalisation capability of artificial intelligence-based solar radiation estimator models using a bio-inspired optimisation algorithm and multi-model approach. *Environ. Sci. Pollut. Res.* **2022**, *29*, 27719–27737. [[CrossRef](#)]
53. Alizamir, M.; Kim, S.; Kisi, O.; Zounemat-Kermani, M. A comparative study of several machine learning based non-linear regression methods in estimating solar radiation: Case studies of the USA and Turkey regions. *Energy* **2020**, *197*, 117239. [[CrossRef](#)]
54. Geshnigani, F.S.; Golabi, M.R.; Mirabbasi, R.; Tahroudi, M.N. Daily solar radiation estimation in Belleville station, Illinois, using ensemble artificial intelligence approaches. *Eng. Appl. Artif. Intell.* **2023**, *120*, 105839. [[CrossRef](#)]
55. Mohammadi, B.; Moazenzadeh, R.; Pham, Q.B.; Al-Ansari, N.; Rahman, K.U.; Anh, D.T.; Duan, Z. Application of ERA-Interim, empirical models, and an artificial intelligence-based model for estimating daily solar radiation. *Ain Shams Eng. J.* **2022**, *13*, 101498. [[CrossRef](#)]
56. Guimerà, R.; Reichardt, I.; Aguilar-Mogas, A.; Massucci, F.A.; Miranda, M.; Pallarès, J.; Sales-Pardo, M. A Bayesian machine scientist to aid in the solution of challenging scientific problems. *Sci. Adv.* **2020**, *13*, 101498. [[CrossRef](#)] [[PubMed](#)]

Disclaimer/Publisher’s Note: The statements, opinions and data contained in all publications are solely those of the individual author(s) and contributor(s) and not of MDPI and/or the editor(s). MDPI and/or the editor(s) disclaim responsibility for any injury to people or property resulting from any ideas, methods, instructions or products referred to in the content.